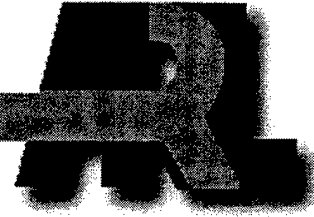*ARMY RESEARCH LABORATORY*

Electrothermal-Chemical (ETC) Closed-Chamber Interrupted-Burning Tests With JA2 and M30 Solid Propellants

by Avi Birk, Miguel Del Guercio, Amy Kinkennon,
Douglas E. Kooker, and Pamela Kaste

ARL-TR-2371   November 2000

DTIC QUALITY INSPECTED 4

20010215 035

Army Research Laboratory

Aberdeen Proving Ground, MD 21005-5066

Electrothermal-Chemical (ETC) Closed-Chamber Interrupted-Burning Tests With JA2 and M30 Solid Propellants

Avi Birk, Miguel Del Guercio, Amy Kinkennon, Douglas E. Kooker, and Pamela Kaste
Weapons and Materials Research Directorate, ARL

Abstract

Interrupted- and noninterrupted-burning tests were conducted with cylindrical perforated grains of JA2 and M30 in a closed bomb with a loading density of approximately 0.2 g/cm³. Both conventional black-powder and plasma igniters were used. The plasma igniter was an ablating capillary, and the electrical energy density was about 0.7 kJ/g of propellant. The diameters of the collected grains yielded the actual burn distance at the time of the interrupted burning. The experimental pressure traces and the conventional burn-rate coefficients of the propellants were used to calculate the theoretical depth burned assuming no plasma-induced burn-rate modifications. Overlapping pressure traces at several interrupted pressures and from comparison to the calculated-versus-measured burn distances indicated that there is burn-rate enhancement during the plasma pulse, but not much once the pulse has ended. In contrast to the JA2 burn rates, both ambient and cold (-20 °C) M30 burn rates, deduced from the noninterrupted tests using the BRLCB code, were enhanced even after the plasma turn-off, thus contradicting the interrupted test results. However, vivacity analysis of the noninterrupted tests indicated that the M30 grains exhibited increased surface area (possible fragmentation) because of the plasma interaction, an effect that would cause erroneous results from the BRLCB. Indeed, simulating the noninterrupted M30 tests using the XNOVAKTC code and assuming partial fragmentation of the propellant charge yielded vivacities that mimicked the experimental ones.

Table of Contents

INTENTIONALLY LEFT BLANK.

List of Figures

INTENTIONALLY LEFT BLANK.

List of Tables

INTENTIONALLY LEFT BLANK.

1. Introduction

The electrothermal-chemical (ETC) closed chamber has been popular as a research tool for studying the effects of plasma-propellant interaction [1–4]. Typically, the chamber is filled with solid-propellant grains at a loading density of about 0.2 g/cm^3, and the propellant is ignited with plasma that is either in the form of a jet generated by an ablating capillary external to the propellant charge [1, 2] or an exploding wire inside the propellant charge [2, 3, 4]. Diagnostics include current and voltage across the capillary or wire and pressure-time history of the gas in the chamber. The electrical power and energy input into the chamber are directly calculated from the current and voltage measurements, but, because of heat losses, less than 75% of the electrical energy actually contributes to the enthalpy increase of the chamber gas [5]. The pressure-time history is analyzed using the U.S. Army Ballistics Research Laboratory Closed Bomb (BRLCB) code [6] that calculates the propellant surface regression rate versus the pressure. The ETC option of the BRLCB code requires the electrical power-time history input. A major input to the code is the geometry of the propellant grains. The code assumes that the instantaneous regression rate and the initial geometry uniquely determine the burning surface. The code output will be erroneous if the burning surface changes because of propellant fracture or fragmentation.

In recent years, regression rates from the ETC closed chamber, as deduced using the BRLCB, have indicated ETC augmentation of the burn rate of solid propellants [1, 2]. Indeed solid-propellant ETC guns achieved performance gains that could not be accounted for by the added electrical energy only—augmentation of the gas-generation rate had to take place. Because the extent of the augmentation has implications with respect to gun performance and its sensitivity to initial propellant temperature [7], it is important to validate the BRLCB results in a more direct method. This augmentation can result from a change in the inherent burn rate of the propellant because of the plasma interaction, or it could be caused by grain fracture or fragmentation that would produce an "unscheduled" increase of burning-surface area. Of course, for gun applications, the desired enhancement mechanism is the one that is most controllable, which favors the inherent burn-rate increase. But Kooker [7], using numerical simulations of gun and closed-bomb firings, hypothesized that most of the apparent gas-generation rates in gun firings and ETC closed chambers could be explained if some degree of grain fragmentation took

place. The present work is about the nature of the burn-rate augmentation, and as is shown, it lends credence to the grain-fracture hypothesis.

The impetus for the present effort was the need to provide extinguished propellant grains that were ignited with plasma of the ablating capillary type for chemical and morphological analysis. Earlier results of some of these analyses were reported by Kaste et al. [8] and are not the subject of this paper. The authors analyze here the measured dimensional change of the extinguished grains and their pressure-time histories to find the plasma effect on the inherent burn rate. In addition, this effort extends Del Guercio's work [1] with noninterrupted burning of ambient M30 and JA2 to the study of cold propellants (-20 °C). Also, the validity of BRLCB-based derivations of the propellant burn rates is checked using vivacity analysis. Applying the BRLCB code, Del Guercio found that the M30 burn rate was significantly augmented, even after the plasma was turned off. Here, Kooker's [7] grain-fracture hypothesis is investigated by applying the XNOVAKTC [9] ballistic code for simulation of partially fragmented M30 burning in the ETC closed chamber and then deriving synthetic vivacities from the simulated pressures. Indeed, the authors find that the synthetic vivacities track well with the experimental ones, which supports Kooker's hypothesis.

2. Experimental

2.1 Test Fixture and Procedure. The experiments were conducted with the ETC closed chamber and pulse-forming network used by Del Guercio [1]. The plasma was generated and sustained by a high-voltage/high-current pulse across a nickel fuse wire, placed along the inside of a capillary, that vaporized rapidly causing ablation and ionization of the polyethylene or Mylar capillary liner. The plasma duration was about 1.2 ms. The electrical pulse was generated with a 400 kJ capacitor-based pulse-forming network with a charging voltage of 4 kV and an output energy of up to 30 kJ.

Closed-bomb tests of M30 and JA2 with both conventional and plasma ignitions were performed in a 3.81-cm-inside diameter (ID) ETC closed chamber with a total volume of 129 cm^3. The chamber was equipped with one or two 607-C4 Kistler pressure transducers. For the interrupted-burning tests, the end plug of the ETC closed chamber was replaced with a plug

containing a stainless steel rupture disc. After rupturing, the disc formed a 2.54-cm opening. A 240-L expansion chamber (a modified air-compressor tank) was interfaced to the ETC closed chamber via a 15-cm-long tube with a 2.5-cm-diameter blowout area. The addition of the interface tube increased the ETC chamber volume to 150 cm^3. A picture of the expansion chamber arrangement is shown in Figure 1.

The propellant charges consisted of seven-perforated grains of M30 or JA2 having a diameter, length, and perforation diameter of approximately 0.75, 1.5, and 0.07 cm, respectively. The charges consisted of either 28 grains (with a total weight of about 30 g) of temperature-conditioned propellants or 30 grains (32 g) at ambient temperature. The grains were packed around a plastic straw and distributed concentrically in two tiers and two rings as pictured in Figure 2 which also shows the charge with respect to the rupture disc. For the tests with the 30 grains, the propellant charge was wrapped with cellophane. For the tests with the 28 grains, the propellant charge was encased in a Styrofoam container that weighed about 0.5 g. In the case of plasma ignition, the plasma was channeled through a plastic straw that was perforated to resemble a piccolo tube to enable uniform distribution of the plasma around the propellant. For conventional ignition, an electric match was used to ignite 0.6 g of black powder confined in a nonperforated plastic straw. The grains extinguished instantly upon sudden expansion into the vacuumed tank. Soft capture of the propellant was achieved with polyurethane foam inside the tank. The absence of burn marks on the foam confirmed the sudden extinguishment.

Temperature conditioning of propellant charges, encased in Styrofoam containers, was done in a temperature conditioner cooled to −65 °C. The charge temperature could not be monitored during the actual test when the charge was sealed in the ETC closed chamber. Therefore, before testing, the warming rates of the propellant charges were calibrated using two thermocouples mounted on the periphery and in the middle of the charge. For each type of propellant, two calibration tests were conducted with the propellant charge mounted, but not sealed, in the ETC chamber. The warming rates were found to be repeatable, and, typically, the charge temperature would rise to −20 °C in about 7.5 min. At that time, the temperature difference between the middle of the charge and its exterior was less than 10 °C. Therefore, in order to test a charge at
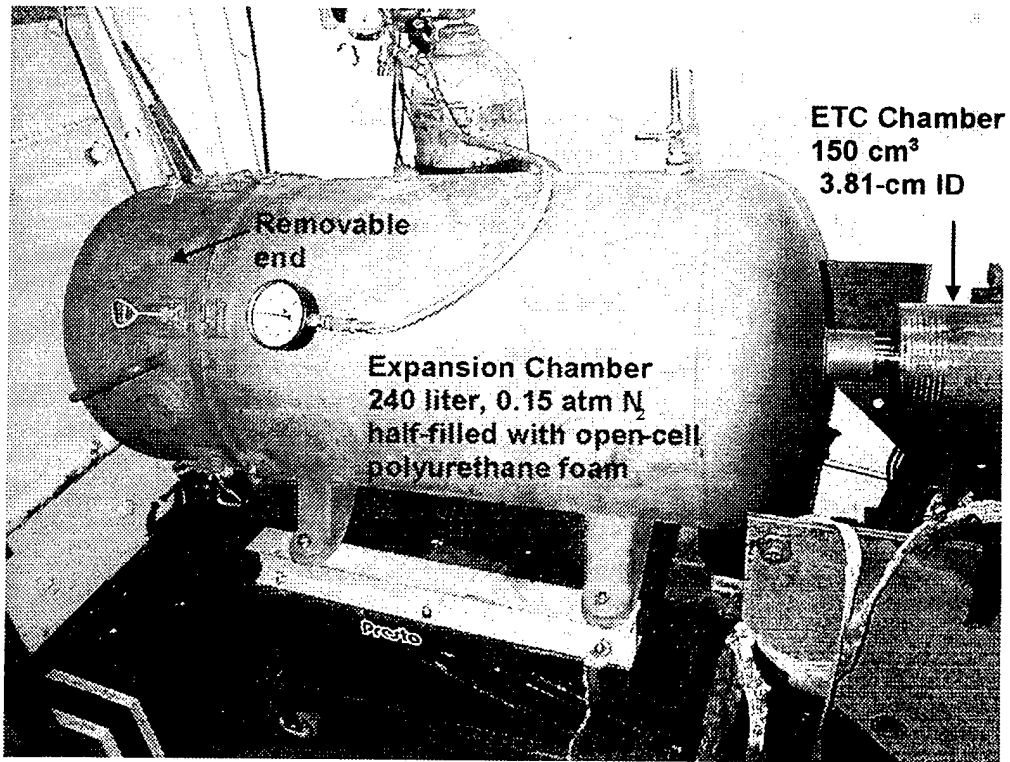
3

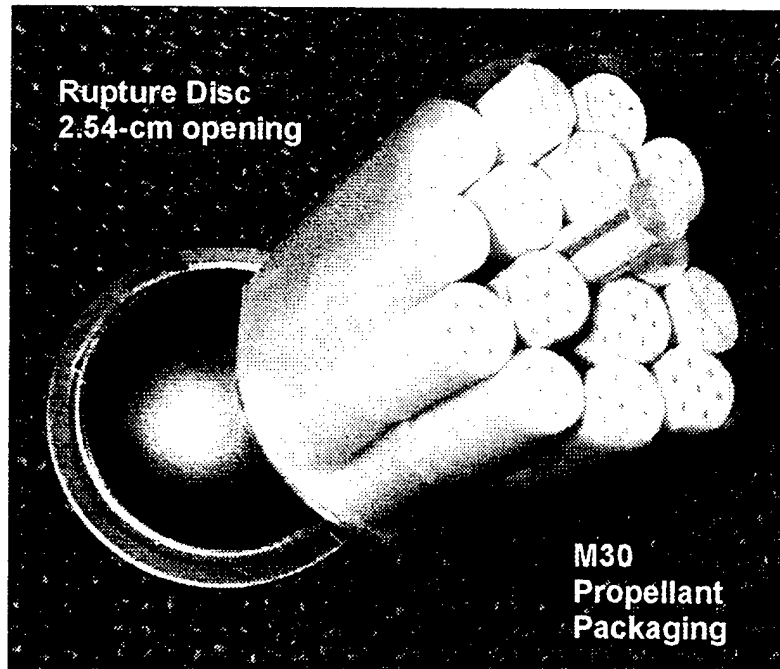Figure 1. Expansion-Chamber Arrangement.

Figure 2. Propellant Packaging.

-20 °C, the igniter had to fire for about 7.5 min from the time the charge was removed from the temperature conditioner.

The goal was to track the original location of the recovered grains to assess whether this location might affect such factors as the quantity or location of residue deposited on the grains, level of decomposition or extent of burning on the grains' surfaces, or any morphological features observed. A simple scoring scheme was devised, which would indicate (1) whether the grain was in the top tier or bottom tier, which is defined as that closest to the igniter; (2) whether the grain was located in the inner or outer ring around the straw, which simulated the piccolo igniter; (3) the end of the grain, which faced downward (i.e., toward the igniter); and (4) the part of the grain that faced radially outward (i.e., away from the igniter). This was accomplished as shown in Figure 3, which shows the appearance of a top tier and bottom grain as viewed end-on from the surface closest to the blow-out disc. A single score was indicative of top-tiered grains; a score through one perforation was used to mark grains adjacent to the straw ("inner" ring, typically 5 grains); and a score through two perforations indicated that the grain was located in the outer ring (typically 10 grains). Two scores indicated that the grains were located in the bottom tier (closest to the igniter). Scores along perforations on consecutive radii indicated that the grains were in the outer packing ring, while those grains with two scores along alternate radii indicated that the grain was packaged adjacent to the straw. The grains were positioned so that the scoring pointed radially outward. Scoring was achieved with a razor and was sufficiently deep to be evident in the recovered grains but did not induce fracture or other artifacts.

After firing, grains were separated according to where they were recovered: remaining in the ETC chamber; loose in the expansion chamber in which the grains were extinguished; or embedded in the polyurethane foam used to line the extinguishing chamber. For each trial, a matrix was established in which the number of grains from each original and final position were recorded.

2.2 Test Matrix. The experimental test matrix is given in Table 1. The tests are ordered chronologically. From test 11 on, Mylar-lined capillaries were used instead of polyethylene

TOP TIER   **BOTTOM TIER**
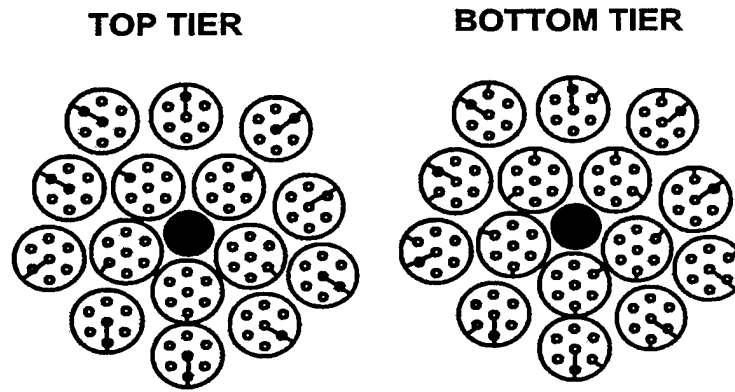
Figure 3. Scoring Scheme Used to Identify the Packaging Position and Orientation of the Grains Prior to Closed-Bomb Analysis.

because they provided somewhat more consistent power-time behavior of the plasma discharge. The Mylar capillaries resulted in less char deposition on the outer surface of the grains and fewer electrical shorts across the electrodes. Moreover, polyethylene consists only of C and H, while Mylar contains C, H, and O; so the effect of ignition chemistry could possibly be compared by chemical analysis of the recovered grains.

The propellants from the "BRL Research Series," dated 1988, and propellant description sheets that included dimensions, compositions, and burn rates were available to the authors. Nevertheless, deviations were found from the described dimensions, and from test 11 on, special care was taken in selecting the grains for the charges. Random M30 grains were found to have dimensional variations of the outer diameter, with a standard deviation of 0.08 mm. The JA2 diameters were better behaved. The standard deviation of the selected grains was about 0.03 mm. The standard deviations of the grains' lengths were above 0.1 mm; hence the lengths were not analyzed. For both propellants, the diameters of the inner perforations were found to be different from those of the outer perforations. Nominal burn rates were initially measured using a 500-cm^3 closed bomb optimized for this purpose. For each propellant, two tests were conducted, and the burn rates were averaged. These are the "nominal burn rates" used to calculate the diameter change in Table 1. The nominal rates for JA2 were very close to the ones in the Research Series; the M30 rates were somewhat different. The closed-chamber method (based on BRLCB) does not give reliable burn rates below 30 MPa. For low pressures, burn-rate

Table 1. Test Matrix

No.	Prop./T[a] Peak Pressure (MPa)	Test Label (left digits are month, day, year)	Calculated[b] Diam. Change (mm)	Measured—Outer Diam., Outer Perf., Inner Perf. (std dev) (mm)	No. of Grains Collected (Tested)	Peak Power (MW), Pulse Width (ms) Capillary	Electric Energy (kJ)
1	M30-Conv/A 80	9108S1P	0.48	0.42, 0.53, 0.51	20 (30)	NA	NA
2	JA2-Conv/A 75	9118S1P	0.508	0.50, 0.47, 0.47	28 (30)	NA	NA
3	JA2-ETC/A 71	9118S2P	0.221	0.270, 0.260, 0.260	20 (30)	28, 1.2 polyethylene	28.1
4	M30-ETC/A 41	9168S1P	0.222	0.365, 0.332, 0.349 (0.044, 0.020, 0.036)	18 (30)	30, 0.5 polyethylene	18
5	M30-ETC/A 41	9168S2P	0.238	0.353, 0.333, 0.340 (0.055, 0.024, 0.036)	23 (30)	24, 0.65 polyethylene	17.2
6	M30-ETC/A 75	9178S1P	0.370	0.380, 0.41, 0.42	15 (30)	24, 1.4 polyethylene	27.4
7	M30-ETC/A 100	9178S2P	0.543	0.66, 0.59, 0.58	12 (30)	25, 1.2 polyethylene	28.5
8	JA2-ETC/A 38	9298S1P	0.081, (0.112[c])	0.183, 0.158, 0.153 (0.039, 0.018, 0.039)	26 (30)	25, 1.2 polyethylene	28.4
9	JA2-ETC/A 93	9298S2P	0.526	0.70, 0.59, 0.58 (0.071, 0.061, 0.097)	13 (30)	25, 1.3 polyethylene	29.4
10	JA2-ETC/A 35	10018S1P	0.167, (0.238[c])	0.280, 0.236, 0.213 (0.045, 0.019, 0.027)	24 (30)	30, 0.7 polyethylene	20
11	M30-ETC/A 59	5119S1P	0.256	0.333, 0.427, 0.392 (0.092)	21 (30)	25, 1.3 Mylar	26.2
12	M30-ETC/A 34.5	5139S1P	0.167	0.230, 0.313, 0.308 (0.090)	28 (30)	25, 0.85 Mylar	18.8
13	M30-ETC/A 78.8	5149S1P	0.478	0.510, 0.600, 0.567 (0.100)	20 (30)	24, 0.95 Mylar	17.7
14	M30-ETC/A 34.4	5179S1P	0.135	0.190, 0.242, 0.244 (0.090)	26 (30)	24, 1.3 Mylar	21.5
15	M30-ETC/A 72.4	5189S1P	0.332	0.466, 0.497, 0.474 (0.073)	21 (30)	27, 1.3 Mylar	28.9
16	M30-Conv/A 36.1	5199S1P	0.390	0.367, 0.424, 0.413 (0.097, 0.043, 0.043)	28 (30)	NA	NA
17	M30-Conv/A 61.9	5209S1P	0.631	0.618, 0.612, 0.619 (0.105, 0.034, 0.065)	23 (30)	NA	NA
18	M30-ETC/A 100.8	5219S1P	0.666	0.760, 0.767, 0.768 (0.09, 0.069, 0.061)	15 (30)	27, 0.85 Mylar	19.8
19	JA2-ETC/C 281.2	5289S1P	NA	NA	NA (28)	26, 1.1 Mylar	26.9
20	JA2-Conv/C 263.2	5289S2P	NA	NA	NA (28)	NA	NA

[a]Propellant-ignition method/propellant temperature: A = 22 ± 2 °C, C = –20 ± 5 °C.
[b]Based on the nominal burn rates: BR (cm/s) = 0.2195 * P(MPa)$^{0.7803}$ for M30.
  BR (cm/s) = 0.1379 * P(MPa)$^{0.9412}$ for JA2.
[c]From Miller's [10] strand burner for JA2 (1–10 MPa): BR (cm/s) = 0.2745 * P(MPa)$^{0.8309}$.
[d]Based on the ETC chamber, test 6119S1P: BR(cm/s) = 0.2525 * P(MPa)$^{0.7519}$.
[e]Based on the ETC chamber, test 6049S1P: BR(cm/s) = 0.2678 * P(MPa)$^{0.7307}$.

Table 1. Test Matrix (continued)

No.	Prop./T[a] Peak Pressure (MPa)	Test Label (left digits are month, day, year)	Calculated[b] Diam. Change (mm)	Measured—Outer Diam., Outer Perf., Inner Perf. (std dev) (mm)	No. of Grains Collected (Tested)	Peak Power (MW), Pulse Width (ms) Capillary	Electric Energy (kJ)
21	M30-Conv/C 251.6	6049S1P	NA	NA	NA (28)	NA	NA
22	M30-ETC/C 275.8	6089S1P	NA	NA	NA (28)	24, 1.3 Mylar	24.6
23	M30-ETC/A 285	6109S1P	NA	NA	NA (28)	26, 1.2 Mylar	24.3
24	M30-Conv/A 253.7	6119S1P	NA	NA	NA (28)	NA	NA
25	M30-ETC/C 106	6149S1P	0.792, (0.808[d]) (0.793[e])	0.866, 0.839, 0.840 (0.098, 0.035, 0.035)	9 (28)	25, 1.2 Mylar	23.3
26	JA2-ETC/C 102.6	6159S1P	0.750	0.813, 0.745, 0.759 (0.075, 0.035, 0.075)	14 (28)	29, 1.3 Mylar	25.9
27	M30-ETC/C 35.1	6169S1P	0.116, (0.134[d]) (0.131[e])	0.222, 0.226, 0.227 (0.040, 0.013, 0.030)	23 (28)	26, 1.3 Mylar	27.2

[a]Propellant-ignition method/propellant temperature: A = 22 ± 2 °C, C = -20 ± 5 °C.
[b]Based on the nominal burn rates: BR (cm/s) = 0.2195 * $P(MPa)^{0.7803}$ for M30.
BR (cm/s) = 0.1379 * $P(MPa)^{0.9412}$ for JA2.
[c]From Miller's [10] strand burner for JA2 (1–10 MPa): BR (cm/s) = 0.2745 * $P(MPa)^{0.8309}$.
[d]Based on the ETC chamber, test 6119S1P: BR(cm/s) = 0.2525 * $P(MPa)^{0.7519}$.
[e]Based on the ETC chamber, test 6049S1P: BR(cm/s) = 0.2678 * $P(MPa)^{0.7307}$.

data from strand-burner tests were considered to be more reliable. For JA2, Miller [10] has obtained sub-10 MPa data that are significantly different from our "nominal" data. Calculated diameter changes, based on Miller's burn-rate coefficients, are given for the low-pressure JA2 (test numbers 8 and 10 in Table 1) to compare to the changes based on the nominal coefficients.

For the interrupted tests, the peak pressure obtained depended on the rupture disc used. Rupture discs with nominal burst pressures of 35 and 70 MPa were used in a single or double-mount configuration. The electrical parameters in Table 1 were intended to be held constant, but the repeatability of the peak power, pulse shape, and pulse width was less than desired.

2.3 Grain Archeology. In the following discussion, the top tier refers to the 15 grains closest to the rupture disc, and the bottom tier refers to the 15 grains closest to the igniter. The closed bomb is referred to as bomb, and chamber refers to the expansion chamber used to interrupt the burning.

8

More grains were recovered when extinguished at 35 MPa than at 60–70 MPa. At 35 MPa, grains remaining in the bomb were primarily from the bottom outer region; grains from the middle all passed through the bomb and entered the chamber and the foam, whether from the top or bottom tiers. At higher pressures, only the bottom outer grains were found in the bomb.

The grains recovered from the plasma-ignited samples were visibly different from the conventionally ignited samples. In the case of plasma-ignited samples, the top were light cream in color, and the bottom were covered with a black residue. The residue was less dense for the Mylar-based capillary samples than for the polyethylene-based capillary samples. The residue appeared mainly on the grains originally located in the bottom tier, nearest the igniter. Conventionally ignited samples (35 MPa) also exhibited some residue, presumably from the black-powder ignition, but the coating was less dense than for the plasma case, and it was mainly limited to the bottom middle grains. The color variations persisted into the higher pressures. The white virgin M30 grains turned to a golden-brown color in the extinguished samples (75 MPa, Figure 4a) from the conventional ignition. In contrast, most recovered grains from the plasma ignition were blackened (100 MPa, Figure 4b). However, the recovered plasma-ignited M30 grains that were shielded from the direct blast of the plasma had a light cream color. The reasons for the color variations are not understood at this time.
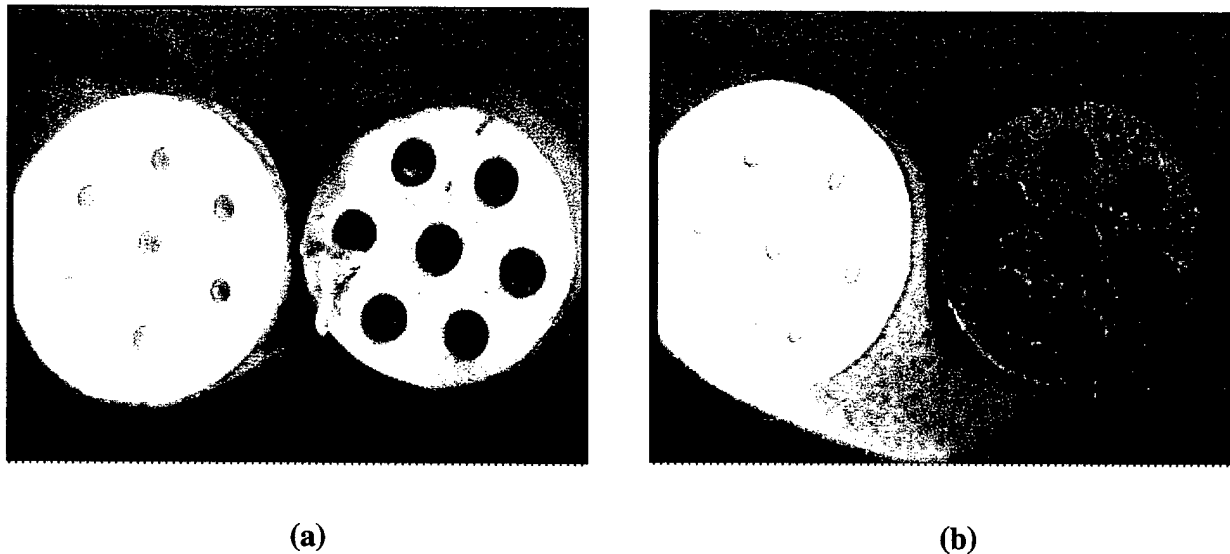

(a)   (b)

Figure 4. Samples: (a) Conventionally Ignited With Black Powder and (b) Plasma-Ignited With Mylar-Based Capillaries.

The top tier grains were all found in either the chamber or the foam. At 35 MPa, those found in the foam were virtually the same color as the virgin material except for areas that had a light coating of black powder residue. In contrast, grains from the same firing but originally located in the outer ring of the bottom tier and recovered in the closed bomb were distinctly yellowed. At 35 MPa, the number of grains remaining in the bomb were comparable for plasma- and black-powder-ignited samples and mainly originated from the bottom tier, middle section. For plasma-ignited samples, these grains had the greatest level of residue from the capillary.

At 62–78 MPa, fewer grains (about 20 of the 30 originally packaged) were recovered for either conventionally or plasma-ignited samples. Most of the recovered grains were from the bottom tier and found in the chamber (not foam). The unrecovered grains primarily originated from the top tier; the top tier grains that were recovered were mainly found in the foam. At this pressure, in most cases no grains remained in the bomb for either ignition system although occasionally one remains. For plasma-ignited samples at 70–78 MPa, most of the top-tier outer ring samples were driven into the foam. In general, most samples embedded in the foam were lighter in color (i.e., not as golden brown) than those found elsewhere in the chamber. In contrast, very few bottom-tier samples were found in the foam, and they tended to be blackened from the plasma residue.

For 100 MPa and ambient temperature, only plasma-ignited trials were performed. There was little recovery from the top tier of grains and none of the middle samples (top or bottom tier). Only bottom, outer grains were found (9 of 10 original), and these were found in the chamber. No samples remained in the bomb at 100 MPa.

2.4 Burn Distances. For the same rupture pressure, burning occurred to a greater extent in the samples ignited with black powder than with the plasma; with the plasma-ignited samples, a significant fraction of the total pressure was due to plasma injection rather than propellant burning. This initial plasma pressurization occurs rapidly, leaving a shorter effective time for propellant burning to occur when compared to conventional ignition (see Figure 5). This occurred whether Mylar or polyethylene capillaries were used in the plasma ignition. This is reflected by the extent of grain regression. For example, for M30 grains recovered nominally at
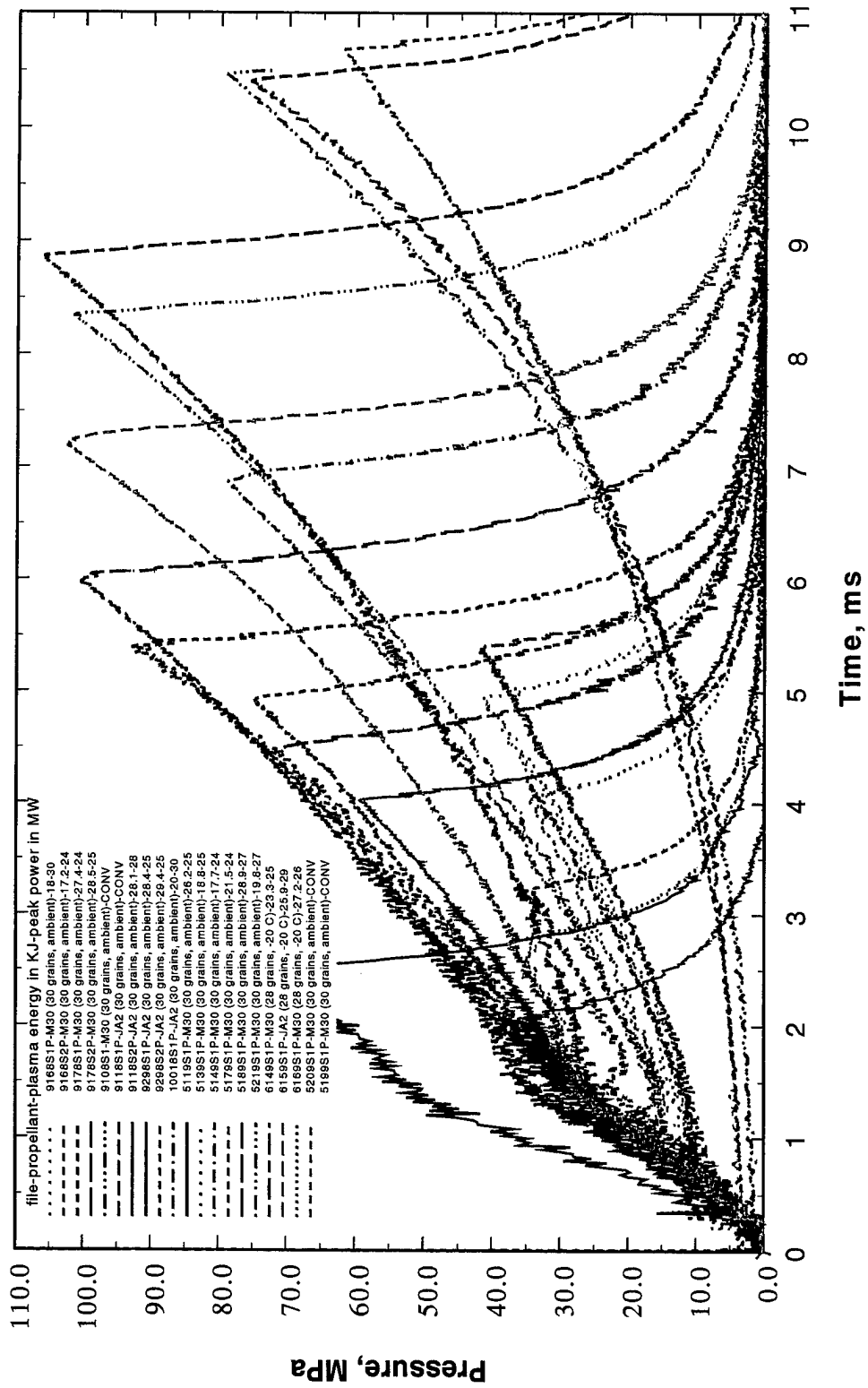
10

Figure 5. Pressure Profiles of the Interrupted-Burning Tests.

35 and 60 MPa, the grain regression measured for plasma-ignited samples (Mylar capillaries) was 0.23 and 0.33 mm, while for conventionally ignited samples, the regression was greater at 0.37 and 0.62 mm, respectively.

The burn distances of the extinguished grains were measured using calipers for the outer diameter and drill bits to gauge the size of the perforations. The outer-diameter burn distances were emphasized more because the burning in the perforations, though their diameters were still small, might have been influenced by erosive flow; the M30 grains were slightly banana-shaped; the set of drill bits had uneven and relatively large size increments; and the drill bits could not always be passed through the perforations. The diameter of each collected propellant grain was measured, and the measurements were averaged. Not all of the grains were found intact. The authors did not find significant burn-distance variances with respect to the packaging locations.

The measured burn distances were compared to theoretical distances calculated from the experimental pressure curves. The method of calculation is demonstrated in Figure 6, where the "nominal" burn-rate coefficients (a, n) are used. If the calculated burn distances are less than 0.08 mm from the measured ones, the authors consider that there is no burn-rate enhancement due to the plasma interaction. If the burn rate has been enhanced, then the calculated burn distance is smaller than the measured burn distance. Figure 6 also demonstrates how to obtain post-plasma burn distances. The figure considers identical propellants fired under similar plasma peak powers and energies for which the pressure-time histories were comparable, with the exception that they were extinguished at two different pressures. Typically, during the plasma pulse, the pressure would rise to about 30 MPa; therefore, comparing calculated regression with the measured propellant regression between two pressures beyond 30 MPa yields the extent of the intrinsic post-ETC burn-rate augmentation. This method circumvents the uncertainty regarding the burn-rate coefficients at pressures below 30 MPa.

The sensitivity of the burn-distance calculations to the assumed burn rates is demonstrated in Table 2 for the three pairs of tests shown in Figure 7. Unfortunately, the experimental power pulse shapes were somewhat variable, and it was a matter of serendipity to obtain both overlapping pressure and power traces. The two electrical power-time histories for the JA2 pair

12

Pressure, (P), MPa

110.0
100.0
90.0
80.0
70.0
60.0
50.0
40.0
30.0
20.0
10.0
0.0

0 1 2 3 4 5 6 7 8 9 10 11

Time, (t), ms

Calculated diameter change due to burning:

$$DC(t) = 2 * \int_0^t a * P(t)^n \, dt$$

For JA2: a = 0.1379, n = 0.9412

At extinguishment:

DC(A) = 0.081 mm ; DC(B) = 0.526 mm

Post ETC diameter change:

DC(B) - DC(A) = 0.445 mm
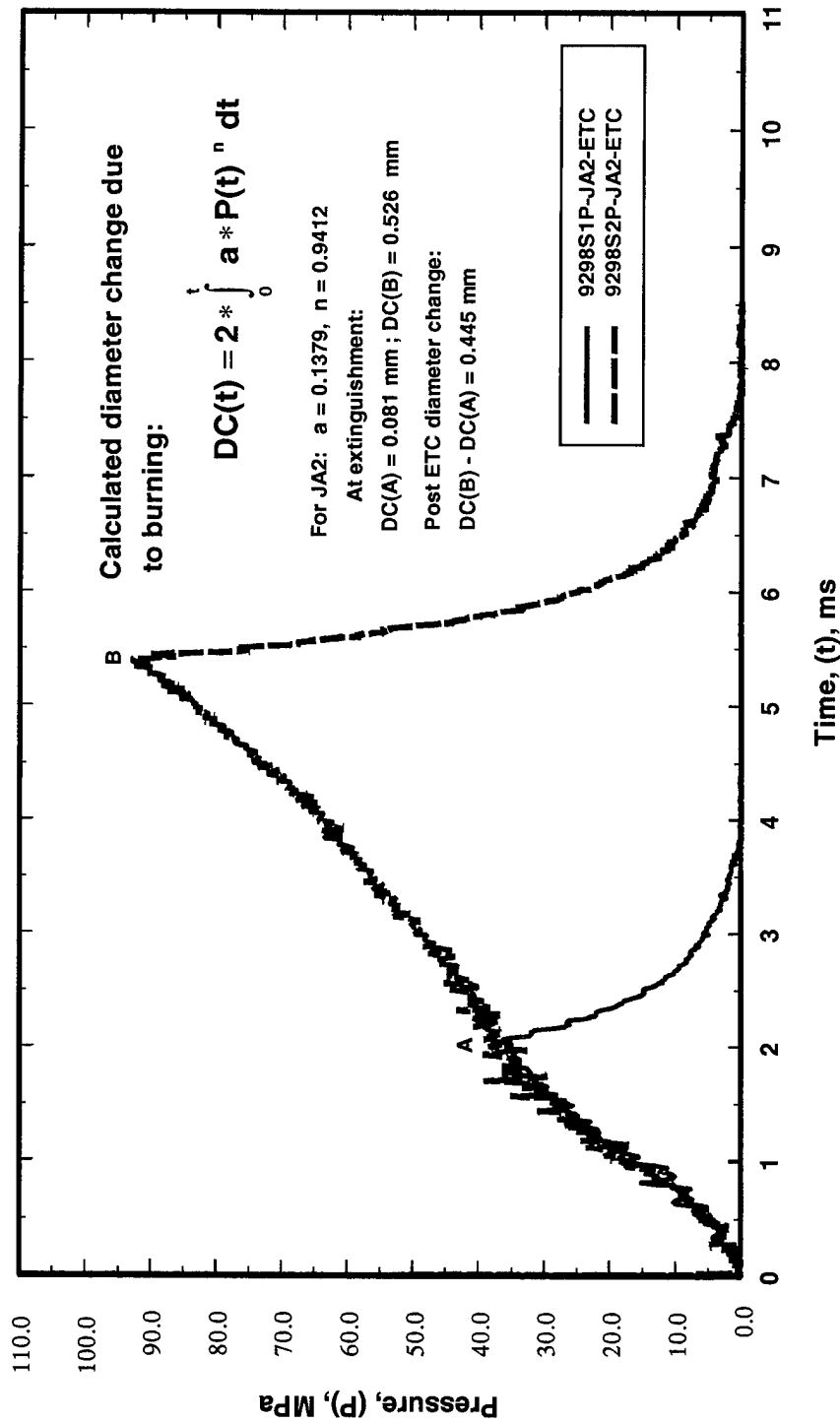
9298S1P-JA2-ETC
9298S2P-JA2-ETC

A

B

Figure 6. Example of Calculation of Burn Distance From Known Burn Rate and Experimental Pressure.

13

Table 2. Sensitivity of Calculated Propellant Diameter Decrease to the Assumed Burn Rate

Conventional Ignition M30 Test	Measured (std dev) (mm)	Nominal Based on 500-cm^3 Closed Chamber $0.2195 * P^{0.7803}$	Based on ETC Chamber Conv. Ignition Test 6119S1P (70–250 MPa) $0.2524 * P^{0.7519}$	Based on 500-cm^3 Closed Chamber (10–73 MPa) $0.2454 * P^{0.7575}$	From Propellant Data Sheet $0.2856 * P^{0.717}$
5199S1P	0.367 (0.097)	0.390	0.422	0.416	0.440
5209S1P	0.618 (0.105)	0.631	0.674	0.661	0.702
Difference	0.251	0.241	0.252	0.245	0.262
—	0.251 - 0.241 = 0.010		—	—	—

Plasma Ignition M30 Test	Measured (std dev) (mm)	Nominal Based on 500-cm^3 Closed Chamber $0.2195 * P^{0.7803}$	Based on ETC Chamber Conv. Ignition Test 6119S1P (70–250 MPa) $0.2524 * P^{0.7519}$	Based on ETC Chamber-ETC Ignition Test 6109S1P (70–250 MPa) $1.039 * P^{0.4736}$	From Propellant Data Sheet $0.2856 * P^{0.717}$
5219S1P	0.760 (0.09)	0.666	0.694	0.978	0.684
5139S1P	0.230 (0.09)	0.167	0.177	0.314	0.183
Difference	0.530	0.499	0.517	0.664	0.501
—	0.530 - 0.499 = 0.031		0.530 - 0.664 = -0.134		—

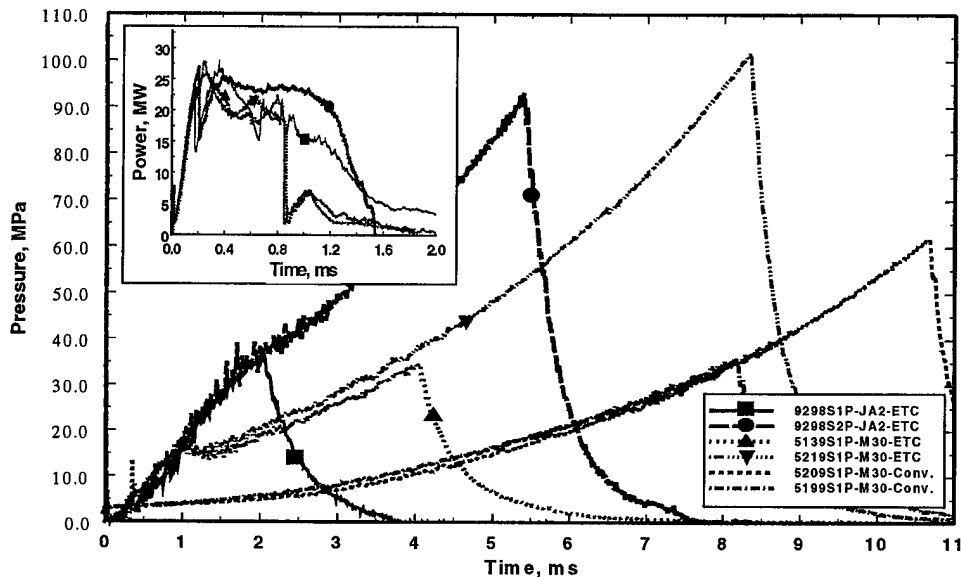| Plasma Ignition JA2 Test	Measured (std dev) (mm)	Nominal Based on 500-cm^3 Closed Chamber $0.1379 * P^{0.9412}$	—	—	From Propellant Data Sheet $0.133 * P^{0.95}$
9298S2P	0.70 (0.071)	0.526	—	—	0.514
9298S1P	0.183 (0.039)	0.081	—	—	0.078
Difference	0.517	0.445	—	—	0.436
—	0.517 - 0.445 = 0.062		—	—	—

Figure 7. Pressure and Power Traces for the Tests of Table 2.

of tests did not overlap as well as the M30 pair of tests. Therefore, although the JA2 pressure traces overlap well, the calculated post-ETC burn distance is less reliable for the JA2 than for the M30. In Table 2, for each pair of tests, the post-ETC regression between the peak pressures is calculated as described in Figure 5. The differences between the measured and calculated post-ETC regressions (e.g., 0.031 mm for M30) are remarkably small—an indication of minimal post-ETC burn-rate enhancement. Table 2 also includes calculations based on burn-rate coefficients obtained (using BRLCB) from noninterrupted tests in the ETC chamber (Figure 8). When coefficients from an M30 ETC test are used, the post-ETC difference between measured and calculated for M30 is too negative (–0.134 mm). Obviously, the BRLCB burn-rate deduction for the M30 ETC test is erroneous.

2.5 Burn Rates Obtained From Noninterrupted Tests in the ETC Closed Chamber.
The burn-rate plots based on the BRLCB code were "wiggly." In the range of 75 to 250 MPa (which is post ETC), when plotted on log-log scale, it became apparent that the plots could be curve-fit to straight lines. The results of the curve fittings are shown in Figure 8. The results for
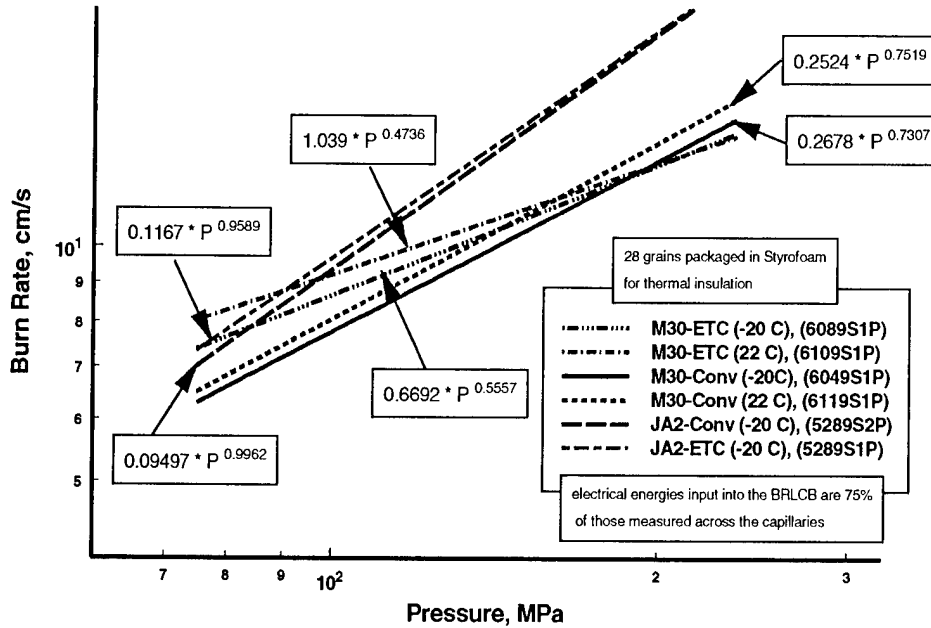
15

Burn Rate, cm/s

10^1
9
8
7
6
5

$0.2524 * P^{0.7519}$

$1.039 * P^{0.4736}$

$0.2678 * P^{0.7307}$

$0.1167 * P^{0.9589}$

28 grains packaged in Styrofoam
for thermal insulation

$0.6692 * P^{0.5557}$

M30-ETC (-20 C), (6089S1P)
M30-ETC (22 C), (6109S1P)
M30-Conv (-20C), (6049S1P)
M30-Conv (22 C), (6119S1P)
JA2-Conv (-20 C), (5289S2P)
JA2-ETC (-20 C), (5289S1P)

$0.09497 * P^{0.9962}$

electrical energies input into the BRLCB are 75%
of those measured across the capillaries

7   8   9 10^2 2   3

Pressure, MPa

Figure 8. Burn Rates From Noninterrupted Tests in the ETC Closed Chamber.

the conventional ignition were close to the results from the 500-cm^3 closed bomb (see Table 2). As expected, ambient M30 burned faster than cold propellant. There was only minor burn rate augmentation for the plasma-ignited JA2, and even this augmentation would disappear if the assumed electrical energy transfer were less than 75%. More importantly, the slopes of the ETC JA2 and conventional JA2 burn-rate curves are virtually parallel. In contrast, the M30 ETC burn rates are markedly enhanced, and the slopes are significantly smaller than those of the conventional M30. As already suggested, the ETC M30 burn-rate curves are inconsistent with the measured grain regression and may be erroneous. This is elaborated upon in section 3.

3. Discussion

3.1 Burn Rates and Vivacity. The technique for calculating vivacity, as applied to closed-chamber pressure data, is well established [11]. Ignoring scaling factors, the vivacity is popularly defined as the instantaneous time derivative of the experimental pressure divided by that pressure. For a certain grain geometry, the plot of the vivacity versus the instantaneous pressure yields a curve with distinct characteristics. For example, a seven-perforated grain like

16

the test propellant should yield a curve that is linear and has a slight positive slope. (The curve is not linear during the ignition/flame-spreading phase and during the final slivering of the grain.) A more energetic propellant (e.g., JA2 versus M30) would yield a steeper curve. The curve has a positive slope if the burning-surface area is progressive and a negative slope if it is regressive. The BRLCB gives reliable burn rates only if the vivacity curve behaves as expected. It is unlikely that changes in the burning-rate pressure indexes (or slopes in Figure 8) are real if the vivacity curves imply unusual changes in burning-surface area. The experimental pressure itself can not reveal much about the burning-surface trends. The contradiction between the measured burn distances and the ones calculated based on the BRLCB results for the ETC M30 led us to plotting the vivacities of the Figure 8 tests. The plots are shown in Figure 9.

Interestingly, the vivacity curves are as expected for all tests save the plasma-ignition tests of the M30 propellant. The experimental vivacities for the M30 ETC tests indicate a regressive burning-surface area. The immediate suspicion is that the more brittle M30 propellant (as compared to JA2) breaks apart to some extent because of the plasma impact, and a few of the M30 grains break into fragments. In order to prove this suspicion, the authors decided to simulate the ETC closed-chamber tests using the XNOVAKTC ballistic code. Input to the code included the "nominal" burn rates (used in Table 2) and simplified experimental power-time histories. The M30 propellant-grain geometry, as well as a combination of "fines" (small spheres, as coined by Kooker [7]) and seven-perforated grains, was inputted. Only 3 or 6 grains out of 28 were converted into fines. The simulated pressure plots from the XNOVAKTC were then processed into synthetic vivacity curves. These curves are shown in Figure 10. The simulated pressures and the synthetic vivacities have somewhat higher values than the experimental ones, but this is mostly because the heat loss routine in the XNOVAKTC underestimates the actual heat loss in the ETC closed chamber. As can be seen, the pressure plots for the conventional versus ETC are markedly different, but the vivacities are quite similar. This is because the vivacity is a measure of the burning-surface geometry. For the case without fines, the ETC vivacities are slightly lower compared to the conventional vivacities. This is just like what was obtained experimentally for JA2 (Figure 9). The synthetic vivacities trend like the experimental M30 vivacities if fines are involved. Therefore, the conclusion was that the ETC M30 experiments involved surface area changes similar to the creation of fines.
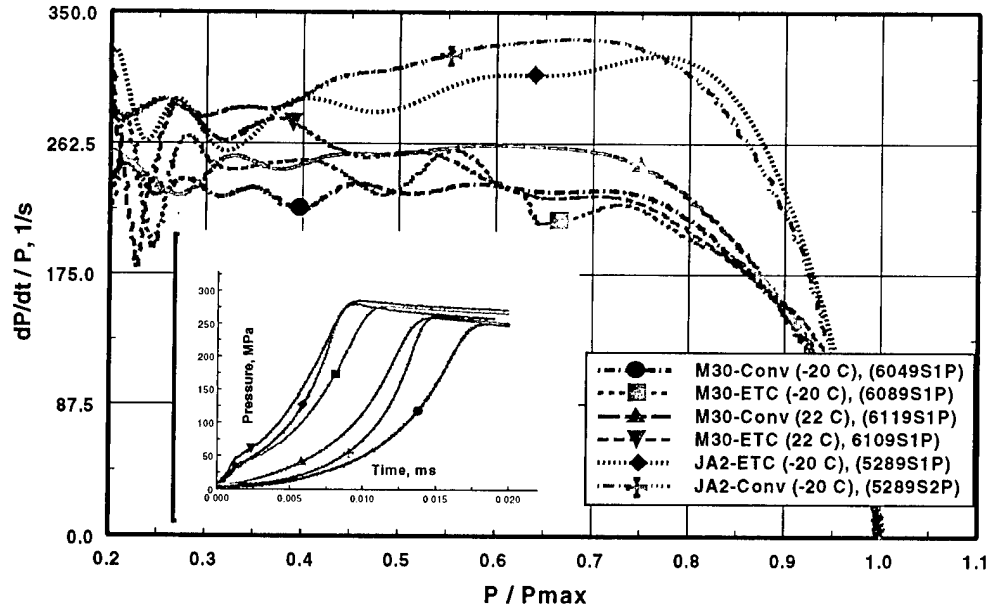
17

Figure 9. Vivacities of the Tests Shown in Figure 8.
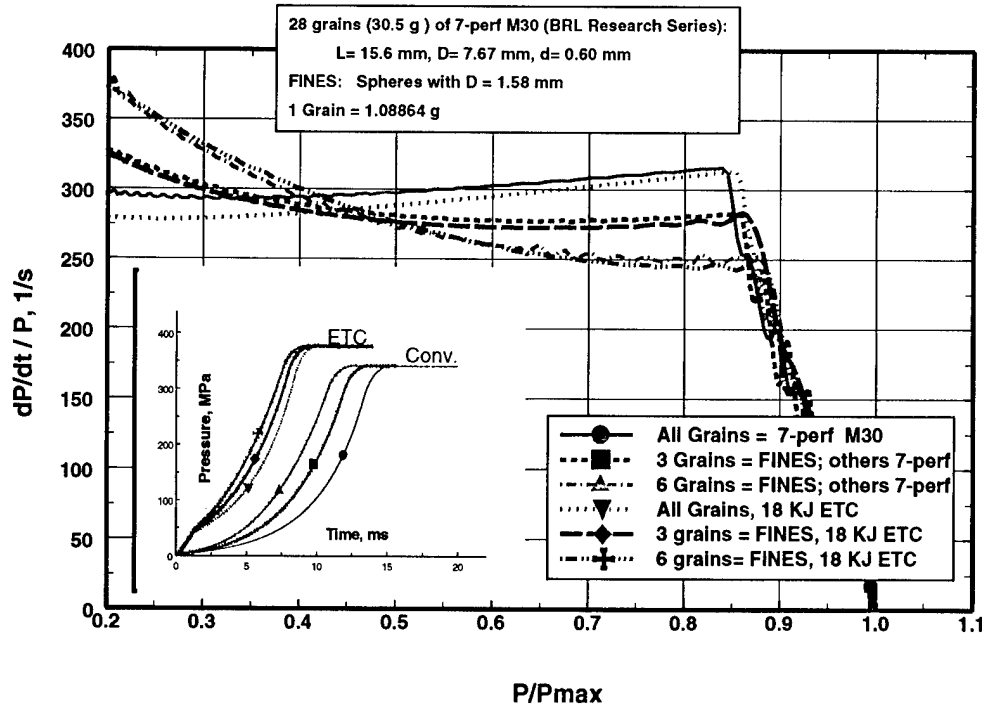

Figure 10. Synthetic Vivacities Based on XNOVAKTC Simulations.

18

The simulated pressures shown in Figure 10 were input into the BRLCB in order to obtain synthetic burn-rate curves for comparison with the experimentally deduced burn rates shown in Figure 8. The burn rates are given in Figure 11. Indeed, the synthetic burn rates, which include a small number of fines, bracket closely the M30-ETC-ambient experimental burn rate. This lends additional support to the propellant-fracture hypothesis.
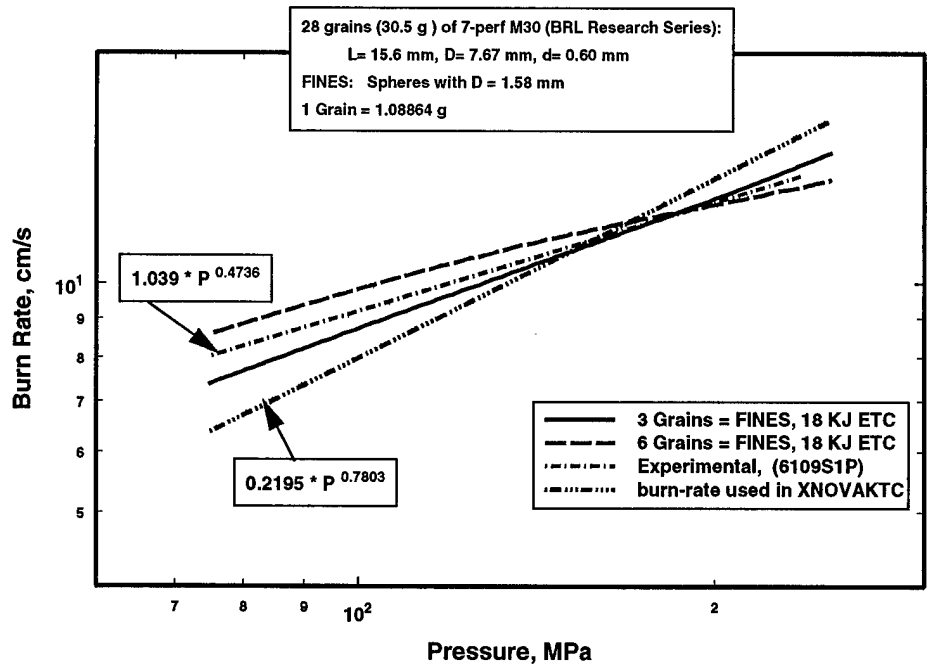
Figure 11. Synthetic Burn Rates Using BRLCB for the Simulated Pressures From the XNOVAKTC.

3.2 Analysis of the Measured Burn Distances. Now that it has been established that, for our test conditions, there is no significant post-plasma burn-rate enhancement, there remains the question of whether there is enhancement during the plasma pulse. For this purpose, the test data of Table 2 were recorded according to "calculated minus measured" (CMM) change of the outer diameter and tabulated in Table 3. First, it is apparent that the conventional CMM is very small and positive while all of the ETC CMMs are negative. The fact that the conventional CMMs are so small bears out the choice for the nominal burn rates assumed in the calculations. The actual

19

ignition of all the grains in the propellant charge is not instantaneous as is assumed in the calculations of the burn distances. If delayed ignition were factored into the calculations, the calculated burn distances would be smaller, and the CMM values would be larger negative numbers falling outside the standard deviation range of the measurements. A negative CMM larger than the standard variation clearly indicates burn-rate enhancement. To investigate burn-rate enhancement during the plasma pulse, we restrict attention to the tests that were interrupted soon after the termination of the plasma (i.e., to peak pressures below 50 MPa). For these tests, the CMM was more negative when the peak power and energy were higher. This is another indication of burn-rate enhancement during the plasma event.

Concentrating on the tests with peak pressures in excess of 50 MPa, we found that the CMMs did not become progressively more negative with progressively higher blowout pressures. This indicates that there is no post-ETC burn-rate enhancement.

3.3 Miscellaneous Observations. The number of grains collected after each test depended on the propellant and the peak pressure. Because M30 is more brittle than JA2, more JA2 grains were collected than M30 grains. Because of higher forces, fewer grains were collected at higher peak pressures. Of particular interest is the number of grains collected at the low peak pressures. At these pressures, the grains are less likely to break during the flow into the expansion/collection chamber. It appeared that fewer ETC M30 grains were collected than conventional M30 grains. For example, test 16 in Table 2 is conventionally fired M30; it reached a peak pressure of 36.1 MPa, and 28 grains out of the original 30 were collected intact. Test 14 is ETC-fired M30; it reached a peak pressure of 34.4 MPa, and 26 grains out 30 were collected. Bearing in mind that the measured burn distance of test 16 is 0.390 mm while the measured burn distance of test 14 is 0.135 mm, the grains of test 16 should have been more fragile than those of test 14 (because of their thinner webs). Yet, more grains were collected in test 16 than in test 14. Also, for the low peak pressures, the number of M30 ETC grains tends to correlate with the peak power—fewer grains were collected at higher peak powers. The above observations are, admittedly, statistically weak; more experiments are needed. Nevertheless, the observations buttress the ETC grain-fracture hypothesis.

20

The capillary material's effect on the burn-rate enhancement could not be determined from the present data. A measure of the ETC burn-rate enhancement is the percent increase of actual burn distance from the calculated burn distance, as given in the right column of Table 3. As the column indicates, soon after the plasma pulse was turned off (i.e., peak pressures below 40 MPa), the enhancement was in the range of 40 to 126%. The fact that the enhancement did not grow progressively with time (and pressure) indicates that little enhancement occurred after the plasma was turned off.

Resources limited the authors to only a few tests with the cold-conditioned grains. Because of increased propellant brittleness at the cold temperature, fewer grains were collected than in the ambient tests with comparable peak pressures. Considering that the propellant-fracture hypothesis is more relevant to brittle propellants, more burn-rate enhancement was expected with cold M30 ETC than with ambient M30 ETC. This did not occur (see Figure 8); perhaps the reason is that lower peak power was obtained in the cold test (see test 22 vs. test 23 in Table 2).

4. Concluding Remarks

The purpose of this effort was to determine the extent that solid-propellant burning rate is modified when interacted with plasma. For this purpose, an ETC closed chamber was used.

The ETC closed-bomb tests employed standard M30 and JA2 propellants having common cylindrical seven-perforated geometries. The plasma was hydrocarbon-based in a form of a jet emanating from a capillary. The electrical density was rather high, about 0.7 kJ/g of propellant. The tests included interrupted and noninterrupted burning, conventional (black-powder) ignition and plasma ignition, and ambient and cold propellants. Test data were in the form of pulse power and pressure traces and measurements of burn distances on extinguished propellants. Data analysis invoked burn-distance calculations, burn-rate deductions using the BRLCB code, vivacity plots, and ballistic simulations using the XNOVAKTC code. Based on the analysis, the following was found:

- There is significant (40–120%) burn-rate enhancement during the plasma pulse.

Table 3. Tests Arranged by CMM of the Outer Diameter

Test Label	Propellant-Ignition Type	Peak Pressure (MPa)	Electrical Energy (kJ)	Peak Power (MW)	Pulse Width (ms)	Capillary	CMM (mm)	-CMM Divided by Calculated Multiplied by 100%
9108S1P	M30-Conv	80	NA	NA	NA	NA	0.060	-12.5
5199S1P	M30-Conv	36.1	NA	NA	NA	NA	0.023	-5.9
5209S1P	M30-Conv	61.9	NA	NA	NA	NA	0.013	-2.1
9178S1P	M30-ETC	75	27.4	24	1.4	Polyethylene	-0.010	2.7
5149S1P	M30-ETC	78.8	17.7	24	0.95	Mylar	-0.032	6.7
5179S1P	M30-ETC	34.4	21.5	24	1.3	Mylar	-0.055	40.7
5139S1P	M30-ETC	34.5	28.8	25	0.85	Mylar	-0.063	37.7
6149S1P	M30-ETC	106	23.3	25	1.2	Mylar	-0.074	9.3
5119S1P	M30-ETC	59	26.2	25	1.3	Mylar	-0.077	100
5219S1P	M30-ETC	100.8	19.8	27	0.8	Mylar	-0.094	14.1
6169S1P	M30-ETC	35.1	27.2	26	1.3	Mylar	-0.106	91.4
9168S2P	M30-ETC	41	17.2	24	0.65	Polyethylene	-0.115	48.3
9178S2P	M30-ETC	100	28.5	25	1.2	Polyethylene	-0.117	21.5
5189S1P	M30-ETC	72.4	28.9	27	1.3	Mylar	-0.134	40.4
9168S1P	M30-ETC	41	18	30	0.5	Polyethylene	-0.143	64.4
9118S1P	JA2-Conv	75	NA	NA	NA	NA	0.008	-1.6
9118S2P	JA2-ETC	71	28.1	28	1.2	Polyethylene	-0.049	22.2
6159S1P	JA2-ETC	102.6	25.9	29	1.3	Mylar	-0.063	8.4
9298S1P	JA2-ETC	38	28.4	25	1.3	Polyethylene	-0.102	126
10018S1P	JA2-ETC	35	20	30	0.7	Polyethylene	-0.113	67.7
9298S2P	JA2-ETC	93	29.4	25	1.3	Polyethylene	-0.174	33.1

- There is no significant burn-rate enhancement in the absence of plasma.

- The plasma-propellant interaction can cause surface-area increase consistent with the hypothesis of grain fracture.

- The above applies also to cold propellants (-20 °C).

The conclusion regarding the fracturing of the grains is not based on truly hard evidence; rather it is based on careful analysis of the data. Mechanisms for the burn-rate enhancement during the plasma interaction will be suggested after the chemical and morphological analysis of the extinguished grains. Based on the findings, burn-rate enhancement should be incorporated during the plasma pulse and/or partial charge fracture in numerical simulations of experimental ETC gun firings.

INTENTIONALLY LEFT BLANK.

5. References

1. Del Guercio, M. "Propellant Burn Rate Modification by Plasma Injection." *34th JANNAF Combustion Subcommittee Meeting*, pp. 35–42, West Palm Beach, FL, 1997.

2. Woodley, C. R., and S. Fuller. "Apparent Enhanced Burn Rates of Solid Propellants Due to Plasmas." *16th International Symposium on Ballistics*, pp. 153–162, San Francisco, CA, 1996.

3. Proud, W. G., and N. K. Bourne. "The Electrothermal Enhancement of Propellant Burning by Plasma Injection." *Propellants, Explosives & Pyrotechnics*, vol. 22, pp. 212–217, 1997.

4. Haak, H. K., A. M. Voronov, and T. H. G. G. Weise. "The Interaction of Electrothermally Supplied Energy With Compact Solid Propellants." *EML Symposium*, Edinburgh, Scotland, 1998.

5. Oberle, W. F., and G. P. Wren. "Radiative and Convective Heat Loss in Electrothermal-Chemical (ETC) Closed Chambers." *35th JANNAF Combustion Subcommittee Meeting*, pp. 229–236, Tucson, AZ, 1998.

6. Oberle, W. F., and D. Kooker. "BRLCB: A Closed-Chamber Data Analysis Program." ARL-TR-36, U.S. Army Research Laboratory, Aberdeen Proving Ground, MD, January 1993.

7. Kooker, D. E. "Burning Rate Deduced From ETC Closed-Chamber Experiments: Implications for Temperature Sensitivity of Gun Systems." *35th JANNAF Combustion Subcommittee Meeting*, pp. 201–217, Tucson, AZ, 1998.

8. Kaste, P. J., A. E. Kinkennon, R. A. Pesce-Rodriguez, M. A. Del Guercio, D. D. Devynck, A. Birk, S. L. Howard, and M. A. Schroeder. "Chemical Analysis of Extinguished Solid Propellants From an Interrupted Closed Bomb With Plasma Igniter." *35th JANNAF Combustion Subcommittee Meeting*, Tucson, AZ, 1998.

9. Gough, P. S. "The XNOVAKTC Code." BRL-CR-627, U.S. Army Ballistics Research Laboratory, Aberdeen Proving Ground, MD, February 1990.

10. Miller, M. Personal communication. U.S. Army Research Laboratory, Aberdeen Proving Ground, MD, 1999.

11. Klingaman K. W., and J. K. Domen. "The Role of Vivacity in Closed Vessel Analysis." *JANNAF Propellant Development and Characterization Subcommittee Meeting*, Patrick AFB, FL, 1994.

INTENTIONALLY LEFT BLANK.

NO. OF COPIES	ORGANIZATION	NO. OF COPIES	ORGANIZATION
2	DEFENSE TECHNICAL INFORMATION CENTER DTIC DDA 8725 JOHN J KINGMAN RD STE 0944 FT BELVOIR VA 22060-6218	1	DIRECTOR US ARMY RESEARCH LAB AMSRL D D R SMITH 2800 POWDER MILL RD ADELPHI MD 20783-1197
1	HQDA DAMO FDT 400 ARMY PENTAGON WASHINGTON DC 20310-0460	1	DIRECTOR US ARMY RESEARCH LAB AMSRL DD 2800 POWDER MILL RD ADELPHI MD 20783-1197
1	OSD OUSD(A&T)/ODDDR&E(R) R J TREW THE PENTAGON WASHINGTON DC 20301-7100	1	DIRECTOR US ARMY RESEARCH LAB AMSRL CI AI R (RECORDS MGMT) 2800 POWDER MILL RD ADELPHI MD 20783-1145
1	DPTY CG FOR RDA US ARMY MATERIEL CMD AMCRDA 5001 EISENHOWER AVE ALEXANDRIA VA 22333-0001	3	DIRECTOR US ARMY RESEARCH LAB AMSRL CI LL 2800 POWDER MILL RD ADELPHI MD 20783-1145
1	INST FOR ADVNCD TCHNLGY THE UNIV OF TEXAS AT AUSTIN PO BOX 202797 AUSTIN TX 78720-2797	1	DIRECTOR US ARMY RESEARCH LAB AMSRL CI AP 2800 POWDER MILL RD ADELPHI MD 20783-1197
1	DARPA B KASPAR 3701 N FAIRFAX DR ARLINGTON VA 22203-1714		ABERDEEN PROVING GROUND
1	NAVAL SURFACE WARFARE CTR CODE B07 J PENNELLA 17320 DAHLGREN RD BLDG 1470 RM 1101 DAHLGREN VA 22448-5100	4	DIR USARL AMSRL CI LP (BLDG 305)
1	US MILITARY ACADEMY MATH SCI CTR OF EXCELLENCE MADN MATH MAJ HUBER THAYER HALL WEST POINT NY 10996-1786		

NO. OF COPIES	ORGANIZATION	NO. OF COPIES	ORGANIZATION

1	DIR ARMY RESEARCH OFFICE
	AMXRO MCS
	K CLARK
	PO BOX 12211
	RESEARCH TRIANGLE PARK NC
	27709-2211
			AMSRL WM BD
			  W ANDERSON
			  P KASTE
			  S BUNTE
			  B FORCH

1	DIR ARMY RESEARCH OFFICE
	AMXRO RT IP LIB SERV
	PO BOX 12211
	RESEARCH TRIANGLE PARK NC
	27709-2211
			AMSRL WM BD
			  A KOTLAR
			  M MCQUAID
			  M MILLER
			  A MIZIOLEK
			  R PESCE RODRIGUEZ
			  J VANDERHOFF

	ABERDEEN PROVING GROUND		AMSRL WM MB R LIEB

40	DIR USARL
	AMSRL WM B
	  A HORST
	  A BARAN
	  B MOORE
	AMSRL WM BA
	  W DAMICO
	AMSRL WM BC
	  M BUNDY
	  P PLOSTINS
	  S WILKERSON
	AMSRL WM BE
	  R ANDERSON
	  A BIRK (5CPS)
	  A BRANT
	  L M CHANG
	  T COFFEE
	  J COLBURN
	  P CONROY
	  M DEL GUERCIO
	  J DESPERITO
	  S HOWARD
	  D KOOKER
	  C LEVERITT
	  T MINOR
	  M NUSCA
	  W OBERLE
	  A WILLIAMS
	  G WREN
	  R BEYER		

REPORT DOCUMENTATION PAGE

1. AGENCY USE ONLY *(Leave blank)*	2. REPORT DATE	3. REPORT TYPE AND DATES COVERED
	November 2000	Final, Sep 98 - Sep 99

4. TITLE AND SUBTITLE

Eletrothermal-Chemical (ETC) Closed-Chamber Interrupted-Burning Tests With JA2 and M30 Solid Propellants

5. FUNDING NUMBERS

NONE

6. AUTHOR(S)

Avi Birk, Miguel Del Guercio, Amy Kinkennon, Douglas E. Kooker, and Pamela Kaste

7. PERFORMING ORGANIZATION NAME(S) AND ADDRESS(ES)

U.S. Army Research Laboratory
ATTN: AMSRL-WM-BE
Aberdeen Proving Ground, MD 21005-5066

8. PERFORMING ORGANIZATION REPORT NUMBER

ARL-TR-2371

9. SPONSORING/MONITORING AGENCY NAMES(S) AND ADDRESS(ES)

10. SPONSORING/MONITORING AGENCY REPORT NUMBER

11. SUPPLEMENTARY NOTES

12a. DISTRIBUTION/AVAILABILITY STATEMENT

Approved for public release; distribution is unlimited.

12b. DISTRIBUTION CODE

13. ABSTRACT*(Maximum 200 words)*

Interrupted- and noninterrupted-burning tests were conducted with cylindrical perforated grains of JA2 and M30 in a closed bomb with a loading density of approximately 0.2 g/cm^3. Both conventional black-powder and plasma igniters were used. The plasma igniter was an ablating capillary, and the electrical energy density was about 0.7 kJ/g of propellant. The diameters of the collected grains yielded the actual burn distance at the time of the interrupted burning. The experimental pressure traces and the conventional burn-rate coefficients of the propellants were used to calculate the theoretical depth burned assuming no plasma-induced burn-rate modifications. Overlapping pressure traces at several interrupted pressures and from comparison to the calculated-versus-measured burn distances indicated that there is burn-rate enhancement during the plasma pulse, but not much once the pulse has ended. In contrast to the JA2 burn rates, both ambient and cold (-20 °C) M30 burn rates, deduced from the noninterrupted tests using the BRLCB code, were enhanced even after the plasma turn-off, thus contradicting the interrupted test results. However, vivacity analysis of the noninterrupted tests indicated that the M30 grains exhibited increased surface area (possible fragmentation) because of the plasma interaction, an effect that would cause erroneous results from the BRLCB. Indeed, simulating the noninterrupted M30 tests using the XNOVAKTC code and assuming partial fragmentation of the propellant charge yielded vivacities that mimicked the experimental ones.

14. SUBJECT TERMS

closed bomb, ETC, interrupted burning, M30 propellant, JA2 propellant, vivacity, burn rate

15. NUMBER OF PAGES

32

16. PRICE CODE

17. SECURITY CLASSIFICATION OF REPORT	18. SECURITY CLASSIFICATION OF THIS PAGE	19. SECURITY CLASSIFICATION OF ABSTRACT	20. LIMITATION OF ABSTRACT
UNCLASSIFED	UNCLASSIFIED	UNCLASSIFIED	UL

INTENTIONALLY LEFT BLANK.

USER EVALUATION SHEET/CHANGE OF ADDRESS

This Laboratory undertakes a continuing effort to improve the quality of the reports it publishes. Your comments/answers to the items/questions below will aid us in our efforts.

1. ARL Report Number/Author___ARL-TR-2371 (Birk)_____Date of Report___November 2000_____

2. Date Report Received_____

3. Does this report satisfy a need? (Comment on purpose, related project, or other area of interest for which the report will be used.) _____

_____

4. Specifically, how is the report being used? (Information source, design data, procedure, source of ideas, etc.)_____

_____

_____

5. Has the information in this report led to any quantitative savings as far as man-hours or dollars saved, operating costs avoided, or efficiencies achieved, etc? If so, please elaborate._____

_____

_____

6. General Comments. What do you think should be changed to improve future reports? (Indicate changes to organization, technical content, format, etc.)_____

_____

_____

_____

                            _____

                            Organization

CURRENT   _____

ADDRESS   Name   E-mail Name

                              _____

                            Street or P.O. Box No.

                              _____

                            City, State, Zip Code

7. If indicating a Change of Address or Address Correction, please provide the Current or Correct address above and the Old or Incorrect address below.

                              _____

                            Organization

OLD   _____

ADDRESS   Name

                              _____

                            Street or P.O. Box No.

                              _____

                            City, State, Zip Code

(Remove this sheet, fold as indicated, tape closed, and mail.)
(DO NOT STAPLE)